International Conference on Applied Energy 2019
Aug 12-15, 2019, Västerås, Sweden
Paper ID: 0720

VALIDATION OF A TWIN-SCREW EXPANDER MODEL WITH EXPERIMENTAL DATA FROM AN ORGANIC RANKINE CYCLE

Fabian Dawo[1*], Sebastian Eyerer[1], Roberto Pili[1], Christoph Wieland[1], Hartmut Spliethoff[1,2]

1 Institute for Energy Systems, Technical University of Munich, Boltzmannstraße 15, 85748 Garching, Germany

2 Bavarian Center for Applied Energy Research, Walther-Meißner-Str. 6, 85748 Garching, Germany

ABSTRACT

Organic Rankine Cycles are a promising technology to generate power from low temperature heat sources and can therefore help to transform current energy systems into renewable ones. However, ORCs are often affected by a broad range of operating conditions; therefore detailed component models are required for the design process. This work validates a semi-empirical model of a twin-screw expander with experimental data from an Organic Rankine Cycle test rig. The results show a satisfying accuracy of the model.

Keywords: Organic Rankine Cycle (ORC), twin-screw expander, modelling, experimental validation

NONMENCLATURE

Abbreviations	
ORC	Organic Rankine Cycle
NPSH	net positive suction head
Symbols	
A	area, m^2
UA	Overall heat transfer factor, W/K
$\dot{m}$	mass flow, kg/s
h	Specific enthalpy, J/kg
n	rotational speed, s^{-1}
p	pressure, bar
P	power, W
$\dot{Q}$	heat flow, W
T	temperature, K
V_i	swept volume intake, m^3
ρ	density, kg/m^3
κ	isentropic exponent, -
ψ	discharge coefficient, -

1. INTRODUCTION

The transformation of current energy systems, mainly based on fossil fuels, into sustainable and renewable ones is currently the main task of energy research. In order to mitigate the effect of climate change, low-temperature/low-enthalpy heat sources like waste heat, biomass, solar heat or geothermal sources should be utilized to produce renewable power and reduce harmful CO_2 emissions. A promising technology to enable these heat sources is the Organic Rankine Cycle (ORC). In contrast to the conventional Rankine Cycle, the ORC employs an organic working fluid instead of water. Organic fluids were historically developed for refrigeration purposes and are characterized by low saturation temperatures compared to water, which allows for higher efficiencies in the case of low temperature heat sources. During the last decades, the ORC concept has been proven and commercialized in many projects. At the end of 2016, the installed capacity of all ORC units worldwide reached around 2700 MW [1]. Nonetheless, several optimization measures can be further investigated to increase the potential of the technology. One major optimization potential is the part-load operation of ORCs because in many cases the ORC plants are subject to variable operating conditions like in geothermal combined heat and power applications [2] or waste heat utilization [3], while the components need to be operated according to their design limits [4]. In order to optimize the design and operational strategies for such ORC units, detailed part-load models of the major components are necessary. This work refines a model first introduced by Lemort et al. [5], who developed it for

Selection and peer-review under responsibility of the scientific committee of the 11th Int. Conf. on Applied Energy (ICAE2019).

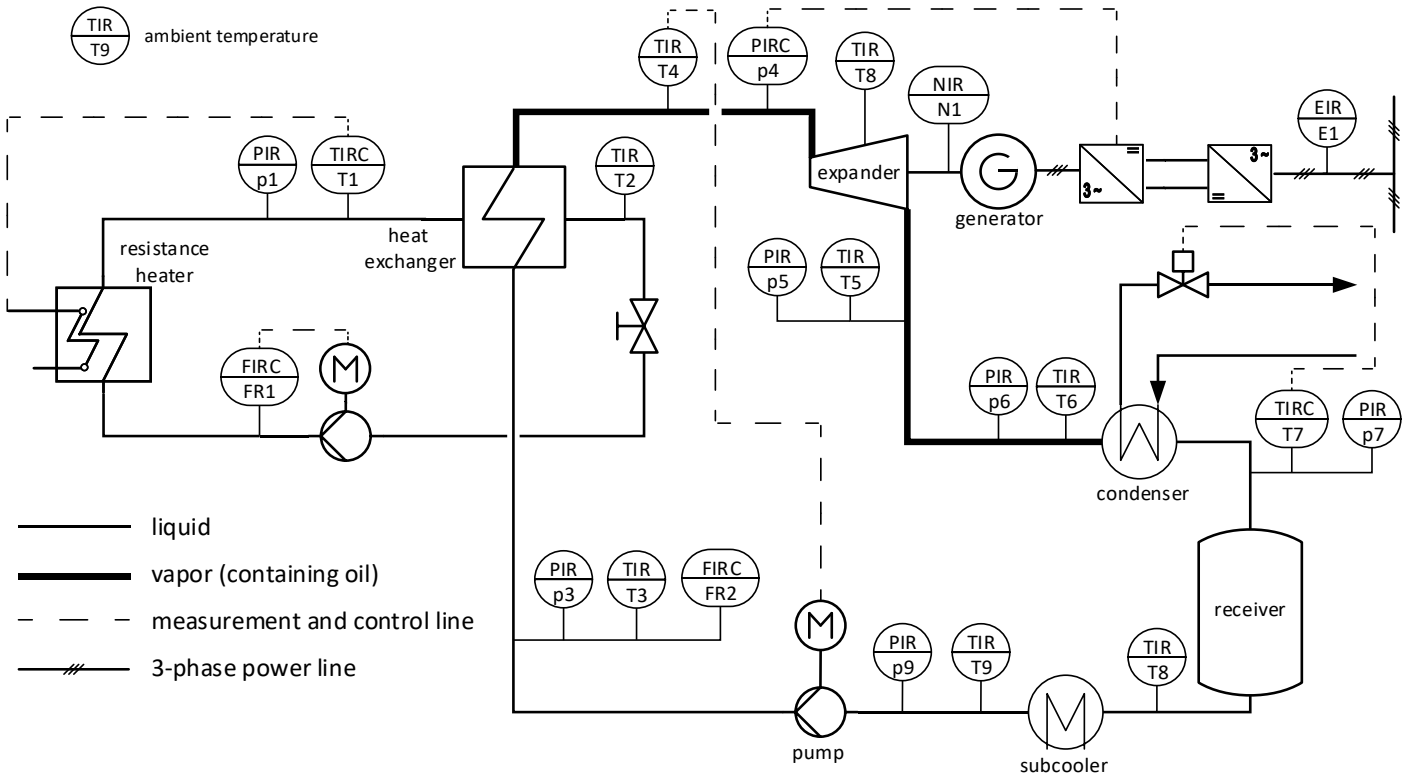

Fig 1 Simplified PID diagram of the ORC test rig with control loops

a scroll expander. The model is then validated with a wide range of experimental data from an ORC test rig, utilizing a twin-screw expander and a novel low GWP working fluid.

2. EXPERIMENTAL SETUP

2.1 Test rig and control loops

Fig 1 shows a simplified piping and instrumentation diagram of the test rig with all major components and the control loops relevant to this work. The test rig is fully instrumented with a temperature and pressure sensor up- and downstream of every major component. Mass and volume flow sensors allow to determine the mass flow in all loops. A water circuit serves as heat source for the ORC. The water is heated by a 200 kW electrical resistance heater, which is controlled to adjust the water temperature. The rotational speed of the circulation pump controls the mass flow in the water loop. The water transfers part of its energy to the working fluid of the ORC in a brazed plate heat exchanger. The working fluid gets thereby preheated, evaporated and superheated. After the heat exchanger, the superheated fluid enters the expander. The expansion machine is an open drive twin-screw volumetric compressor from Bitzer (OSN5361-K), operated in reverse mode. It has a built in volume ratio of 3.1 and a swept volume of 0.678 l on the low-pressure side. The expander shaft is directly coupled to a generator, which produces electricity. The expanded working fluid consecutively flows to the condenser, which is a brazed plate heat exchanger as well. A local cooling water grid is utilized as heat sink for the ORC and condenses the working fluid. The condensed working fluid is fed to a 30 l receiver tank, which supplies the circulation pump of the ORC. In order to ensure the required NPSH of the pump, the saturated working fluid is slightly subcooled in a third brazed plate heat exchanger by tapped water. The degree of superheating of the expander inlet vapor and consecutively the working fluid mass flow is controlled by the rotational speed of the circulation pump. The evaporation pressure can be adjusted to the required value by controlling the rotational speed of the expander. Furthermore, a valve in the cooling water line allows to control the condensation temperature.

2.2 Methodology of experiments

For the validation of the screw-expander model, 38 stationary operating points were investigated, which cover a wide range of operating conditions of the expander. The working fluid was R1233zdE, which is a promising low GWP alternative to R245fa. The heat source supply temperature as well as the condensation temperature were controlled to constant values of 140 °C and 40 °C in all experiments. Fig 2 shows the

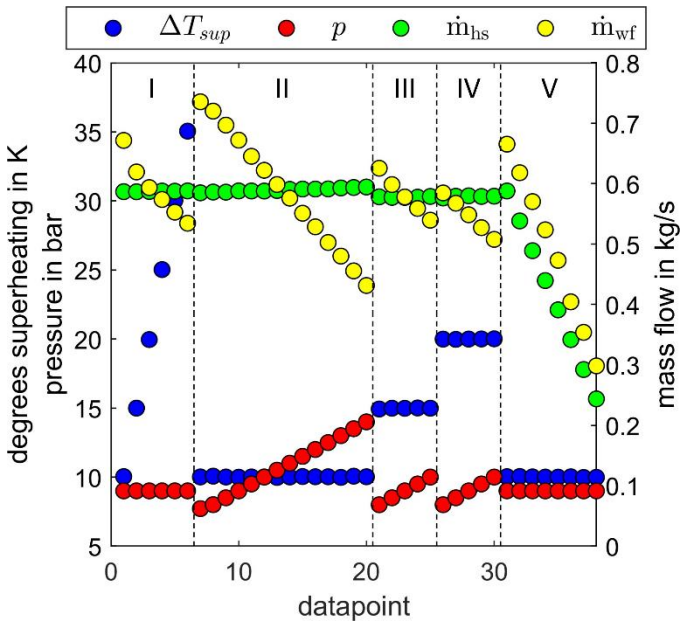

Fig 2 Experimental data

variations in superheating, expander inlet pressure, working fluid mass flow and heat source mass flow for all experiments. The rotational speed of the expander is controlled accordingly. The dashed vertical lines divide the data in five measurement series. In Series I, the mass flow rate of working fluid is decreased at a fixed live vapor pressure, resulting in an increase in superheating. Series II increases the live vapor pressure at constant superheating by reducing the working fluid mass flow. Series III and IV repeat Series II at higher degrees of superheating. For series V, the heat source mass flow is reduced stepwise with constant superheating and pressure, achieved by reducing the mass flow of working fluid.

3. TWIN-SCREW EXPANDER MODEL

The modelling of the twin-screw expander is shown conceptually in Fig 3. The model describes the flow through the expander in three steps, which are described in the following.

3.1 Splitting of inlet mass flow in leakage and internal mass flow

First, the inlet mass flow is split into two streams: an internal stream, which actually produces the shaft power during the expansion process and a leakage stream, which is expanded isenthalpic to the discharge port. The leakage occurs due to gaps between the housing and the rotors and gaps between the two rotors themselves [6]. All leakage paths sum up to a theoretical cross-sectional area and the leakage mass flow is calculated as the mass

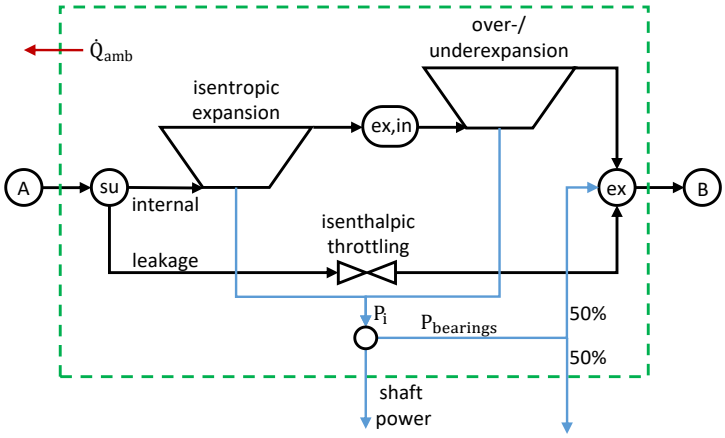

Fig 3 Scheme of the expander model

flow through a nozzle with area A_{leak}:

$$\dot{m}_{leak} = A_{leak} \cdot \psi \cdot \sqrt{2 \cdot p_{su} \cdot \rho_{su}} \quad (1)$$

The discharge coefficient ψ is calculated depending on the flow being either sub- (2) or supersonic (3):

$$\psi = \begin{cases} \left(\frac{2}{\kappa_{su}+1}\right)^{\frac{1}{\kappa_{su}-1}} \cdot \sqrt{\frac{\kappa_{su}}{\kappa_{su}+1}} & (2) \\ \sqrt{\frac{\kappa_{su}}{\kappa_{su}-1} \cdot \left[\left(\frac{p_{ex}}{p_{su}}\right)^{2/\kappa_{su}} - \left(\frac{p_{ex}}{p_{su}}\right)^{\kappa_{su}/(\kappa_{su}+1)}\right]} & (3) \end{cases}$$

The internal mass flow is derived from the geometry of the expander:

$$\dot{m}_{int} = n \cdot V_i \cdot \rho_{su} \quad (4)$$

3.2 Expansion process

The internal mass flow is expanded theoretically isentropically in the machine, given the machine built-in volume ratio. From this process, an isentropic pressure at discharge arises. Depending on whether the expander outlet pressure is lower or higher than the isentropic pressure, over- or under-expansion terms contribute to the internal power:

$$P_i = \dot{m}_{int} \cdot \left[(h_{su} - h_{ex,in}) + \frac{1}{\rho_{ex,in}} \cdot (p_{ex,in} - p_{ex})\right] \quad (5)$$

3.3 Mixing of leaking and internal flow and energy balance

Last, leakage and internal mass flow are mixed before leaving the expander. The energy balance indicated by the dashed green line in Fig 3 has to be satisfied.

$$0 = \dot{m}_A \cdot (h_A - h_B) - \dot{Q}_{amb} - P_i + 1/2 \cdot P_{bearings} \quad (6)$$

The mechanical losses due to friction in the expander bearings $P_{bearings}$ are calculated with manufacturer correlations. The model assumes that half of these losses

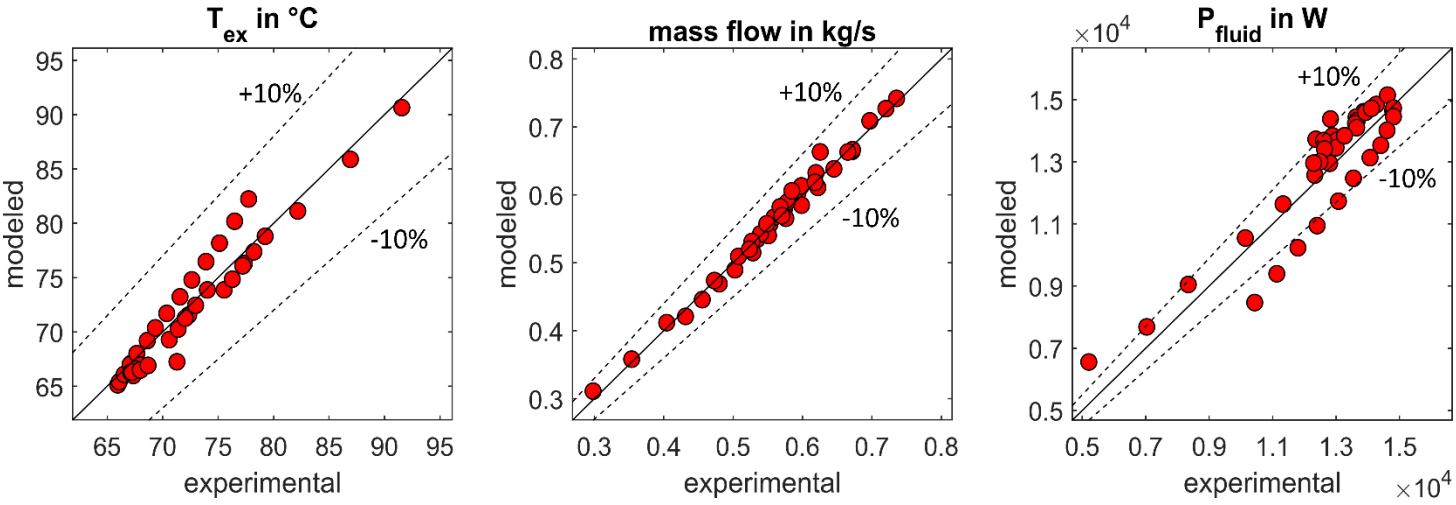

Fig 4 Parity plot for exhaust temperature, working fluid mass flow and fluid power

is dissipated into the exhaust stream and the other half is released to the environment via the shaft. The ambient heat losses are calculated as a heat flow between the expander surface and the surrounding air:

$$\dot{Q}_{amb} = UA_{amb} \cdot (T_{surf} - T_{amb}) \quad (7)$$

4. VALIDATION OF THE MODEL AND DISCUSSION

In order to validate the model with the available experimental data, the cross sectional area A_{leak} of the leakage stream and the overall heat transfer factor UA_{amb} have been fitted in order to minimize the sum of the relative mean square root errors of the exhaust temperature, working fluid mass flow and fluid power, where the fluid power is defined as:

$$P_{fluid} = \dot{m}_A \cdot (h_A - h_B) \quad (8)$$

Fluid power is suitable as a fitting criterion because it incorporates working fluid mass flow and expander outlet temperature, which are the main output values of the model. The optimized value for the leakage area is 3.23e-5 m^2 and 42.40 W/K for the overall heat transfer factor. Fig 4 shows the parity plots for modeled and experimental data. For a perfect model, all points would end up on the black continuous line. Data points above the line indicate that the model overestimates the experimental value and vice versa for points below the line. The dotted lines represent +/- 10% deviation from the perfect fit. The figure shows a satisfying agreement between model and experimental data with almost all data points within 10% deviation. Only for the fluid power, some points slightly exceed these limits.

5. CONCLUSIONS AND OUTLOOK

In order to validate the model of a twin-screw expander, extensive experimental measurements were carried out on an ORC test rig. These data were then utilized to fit the parameters of the semi-empirical model affecting the internal leakage flow and ambient heat loss. The validation of the model showed good agreement with the experimental data. In the future, the model will be extended to predict the mechanical and electrical losses in generator and inverter, the expansion process of partially evaporated fluids and two-stage expansion with vapor extraction.

ACKNOWLEDGEMENT

Funding from the Bavarian State Ministry of Education, Science and the Arts in the framework of the project Geothermal-Alliance Bavaria is gratefully acknowledged.

REFERENCES

[1] Tartière T, Astolfi M. A World Overview of the Organic Rankine Cycle Market. Energy Procedia 2017;129:2–9.

[2] Dawo F, Wieland C, Spliethoff H. Kalina power plant part load modeling: Comparison of different approaches to model part load behavior and validation on real operating data. Energy 2019;174:625–37.

[3] Pili R, Romagnoli A, Jiménez-Arreola M, Spliethoff H, Wieland C. Simulation of Organic Rankine Cycle – Quasi-steady state vs dynamic approach for optimal economic performance. Energy 2019;167:619–40.

[4] Eyerer S, Dawo F, Rieger F, Schuster A, Aumann R, Wieland C et al. Experimental and numerical investigation of direct liquid injection into an ORC twin-screw expander. Energy 2019;178:867–78.

[5] Lemort V, Quoilin S, Cuevas C, Lebrun J. Testing and Modeling a Scroll Expander Integrated into an Organic Rankine Cycle. Applied Thermal Engineering 2009;29(14-15):3094–102.

[6] Macchi E, Astolfi M (eds.). Organic Rankine Cycle (ORC) Power Systems: Woodhead Publishing; 2017.